

## A new neural network approach to density calculation on ceramic materials

Vojislav V. Mitic<sup>\*,†,¶</sup>, Srdjan Ribar<sup>‡</sup> and Branislav M. Randjelovic<sup>\*,§</sup>

<sup>\*</sup>*Faculty of Electronic Engineering, University of Nis, Nis, Serbia*

<sup>†</sup>*Institute of Technical Sciences, Serbian Academy of Sciences and Arts,  
University of Belgrade, Belgrade, Serbia*

<sup>‡</sup>*Faculty of Mechanical Engineering, University of Belgrade, Belgrade, Serbia*

<sup>§</sup>*Faculty of Teachers Education, University of K. Mitrovica, Leposavic, Serbia*

<sup>¶</sup>*vmitic.d2480@gmail.com*

Dejan Aleksic

*Faculty of Science, University of Nis, Nis, Serbia*

Hans Fecht

*Institute of Functional Nanosystems, University of Ulm, Ulm, Germany*

Branislav Vlahovic

*North Carolina Central University (NCCU), Durham, NC, USA*

Received 13 August 2021

Revised 7 October 2021

Accepted 10 October 2021

Published 17 November 2021

The materials' consolidation, especially ceramics, is very important in advanced research development and industrial technologies. Science of sintering with all incoming novelties is the base of all these processes. A very important question in all of this is how to get the more precise structure parameters within the morphology of different ceramic materials. In that sense, the advanced procedure in collecting precise data in submicro-processes is also in direction of advanced miniaturization. Our research, based on different electro-physical parameters, like relative capacitance, breakdown voltage, and  $\tan\delta$ , has been used in neural networks and graph theory successful applications. We extended furthermore our neural network back propagation (BP) on sintering parameters' data. Prognosed mapping we can succeed if we use the coefficients, implemented by the training procedure. In this paper, we continue to apply the novelty from the previous research, where the error is calculated as a difference between the designed and actual network output. So, the weight coefficients contribute in error generation. We used the experimental data of sintered materials' density, measured and calculated in the bulk, and developed possibility to calculate the materials' density inside of consolidated structures. The BP procedure here is like a tool to come down between the layers, with much more precise

<sup>¶</sup>Corresponding author.

materials' density, in the points on morphology, which are interesting for different microstructure developments and applications. We practically replaced the errors' network by density values, from ceramic consolidation. Our neural networks' application novelty is successfully applied within the experimental ceramic material density  $\rho = 5.4 \times 10^3$  [kg/m<sup>3</sup>], confirming the direction way to implement this procedure in other density cases. There are many different mathematical tools or tools from the field of artificial intelligence that can be used in such or similar applications. We choose to use artificial neural networks because of their simplicity and their self-improvement process, through BP error control. All of this contributes to the great improvement in the whole research and science of sintering technology, which is important for collecting more efficient and faster results.

*Keywords:* Ceramics; sintering; neural network; error; density.

## 1. Introduction

This paper deals with ceramic material samples, consolidated by the sintering data obtained in the analyzed experiment. For this purpose, back propagation (BP) neural networks are used. This type of neural network is practically input-output data mapping due to a large set of adjustable coefficients, called weights. By setting the coefficients to appropriate values, it is possible to achieve a desired mapping. Such a procedure is called the training of neural networks. If we start with random values of weights, the training process input-output training data are set to a network and the desired mapping is known.

If the weight values are inappropriate, then mapping will be performed with errors, i.e. the difference between the desired and actual output. Each of the weight coefficients has a significant contribution to the error. By changing the coefficients, through the process of neural network training, the error decreases and the network mapping will be satisfactory for any new input data set, because the network is trained. The training process is over when all input-output data are mapped within a predefined error. This process is called error BP, since it performs output to input.<sup>1-4</sup>

This paper extends the application of neural networks on the sintering and calculation of various parameters, within different sintering temperatures' intervals. The process of consolidation of the ceramic materials at different thermal conditions is very important for density. The neural networks (shown on Fig. 1) are an efficient tool for the calculation of different physical parameters of ceramic materials. From the experimental point of view, because if applied to measurement results, it fits

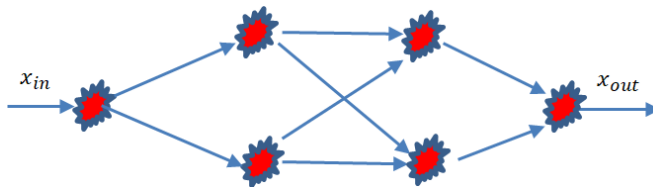


Fig. 1. (Color online) An example of neural network.

Table 1. Extract of experimental results.

Sample type	$P$ [MPa]	$r$ [kg/m <sup>3</sup> ]
BaTiO <sub>3</sub> — ceramics with basic mixture	86	$5.4 \times 10^3$
BaTiO <sub>3</sub> — ceramics: composition 0.1%CeO <sub>2</sub> +0.14%MnCO <sub>3</sub>	86	$3.2 \times 10$
BaTiO <sub>3</sub> — ceramics: composition 0.1%CeO <sub>2</sub> +0.14%MnCO <sub>3</sub>	86	$3.4 \times 10$

extended experimental intervals. There are many different mathematical tools or tools from the field of artificial intelligence that can be used in such or similar applications. We choose to use artificial neural networks because of their simplicity and their self-improvement process, through BP error control. It is interesting to use some other techniques or other tools for modeling and to compare it with the results obtained with the artificial neural network approach. Any signal measured on the material surface could be propagated through the whole structure of the neural network, which is analyzed in Refs. 5–7. Relative capacitance, measured on a sample surface, was propagated through the ceramic structure assuming that the ceramic structure can be presented by a neural network. One of the experimentally obtained parameters is the density of the sintering material, measured on a surface. In order to investigate a possibility to calculate the density of a sintered material within a sintered structure, we used the neural networks, as in Refs. 8–11. The BP training procedure is used as a tool to spread the values measured on a sample surface density. In this research, the network errors are replaced with the density values obtained in the sintering process (Table 1, first row,  $r = 5.4 \times 10^3$  [kg/m<sup>3</sup>]).

## 2. Experimental Results and Methods

There were four steps in the ceramic powder preparation process (for sintering consolidation of BaTiO<sub>3</sub> ceramic samples): (a) measuring and forming starting powders' mixture, (b) wet mixing and spraying, (c) molding and process control and (d) preparation, samples' sintering and process control. The whole the process is applied to a high purity commercial BaTiO<sub>3</sub> Murata powder,<sup>12</sup> with a mean grain size of  $< 2 \mu\text{m}$  and 99.9% purity. The duration of homogenization of organic binders in the powder mixture is about 48 h. Processed into a mill with balls and water, the mass was transferred by a membrane pump and dried, so desired powder granulation was obtained. The material density was tested every hour by a special vessel and after that we applied vibrating sieve. The diameters of roughly shaped powder particles were 10–130  $\mu\text{m}$ .

Various sintering temperatures (1190–1370°C), the length of time (2–3 h) and the impact of different additives (CeO<sub>2</sub>, MnCO<sub>3</sub>, Bi<sub>2</sub>O<sub>3</sub>, and Fe<sub>2</sub>O<sub>3</sub>) are analyzed, but in this analysis we were focused on the relation with pressures of 86 MPa and density.

In further analysis and theoretical experiment, we will use just particular data  $r = 5.4 \times 10^3$  [kg/m<sup>3</sup>], from the first row of the Table 1.

### 3. Theoretical Experiment and Neural Network Method Application

We will develop several different two-layer neural networks, with  $n = 1, 2, 3, 4, 5$  neurons in the first hidden layer and  $m = 1, 2, 3, 4, 5$  neurons in the second hidden layer. For each case, we will discuss the density  $\rho$  in the hidden layers and the errors calculated during the training process:

- For a neural network with one neuron in each of the two hidden layers (Fig. 2), the density  $\rho$  and errors calculated in the training process are given in Table 2.

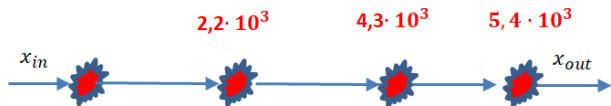


Fig. 2. (Color online) Neural network with one neuron in each hidden layer.

Table 2. Neural network with two neurons in first and one neuron in second hidden layer.

Neuron	Density $\rho$			Errors calculated		
	First hidden layer	Second hidden layer	Output neuron	First hidden layer	Second hidden layer	Output neuron
1	2200	4300	5400	0.076786	0.141702	0.185405

For a neural network with two neurons in the first hidden layer and one neuron in the second hidden layer (Fig. 3), the density  $\rho$  and errors calculated in the training process are given in Table 3.

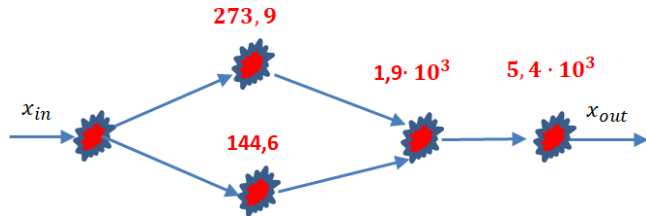


Fig. 3. (Color online) Neural network with two neurons in first hidden layer and one neuron in second hidden layer.

Table 3. Neural network with two neurons in first and one neuron in second hidden layer.

Neuron	Density $\rho$			Errors calculated		
	First hidden layer	Second hidden layer	Output neuron	First hidden layer	Second hidden layer	Output neuron
1	273.9	1900	5400	0.023776	0.314802	0.887293
2	144.6			0.045009		

For a neural network with two neurons in each of the two hidden layers (Fig. 4), the density  $\rho$  and errors calculated in the training process are given in Table 4.

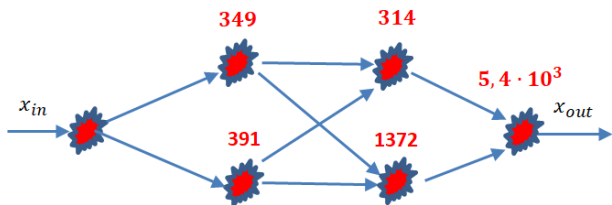


Fig. 4. (Color online) Neural network with two neurons in each hidden layer.

Table 4. Neural network with two neurons in first and one neuron in second hidden layer.

Neuron	Density $\rho$			Errors calculated		
	First hidden layer	Second hidden layer	Output neuron	First hidden layer	Second hidden layer	Output neuron
1	349	314	5400	-0.0654	-0.2297	0.903708
2	391	1372		-0.05848	-0.05259	

For a neural network with three neurons in the first hidden layer and one neuron in the second hidden layer (Fig. 5), the density  $\rho$  and errors calculated in the training process are given in Table 5.

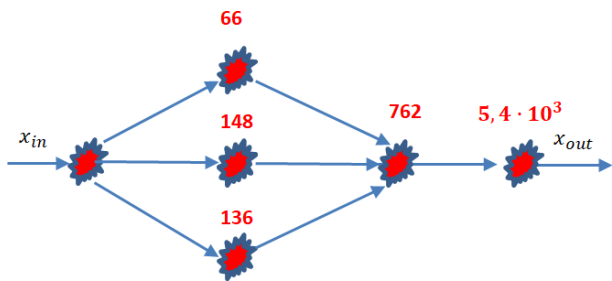


Fig. 5. (Color online) Neural network with three neurons in first hidden layer and one neuron in second hidden layer.

Table 5. Neural network with three neurons in first and one neuron in second hidden layer.

Neuron	Density $\rho$			Errors calculated		
	First hidden layer	Second hidden layer	Output neuron	First hidden layer	Second hidden layer	Output neuron
1	66	762	5400	-0.027	-0.15122	1.071798
2	148			-0.02943		
3	136			-0.01321		

For a neural network with three neurons in the first hidden layer and two neurons in the second hidden layer (Fig. 6), the density  $\rho$  and errors calculated in the training process are given in Table 6.

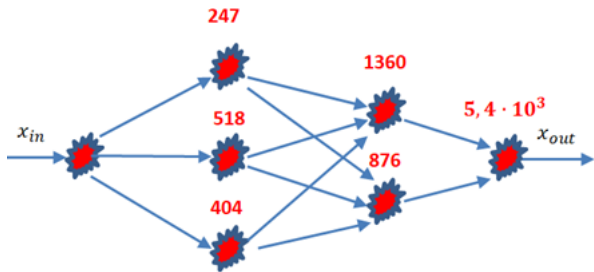


Fig. 6. (Color online) Neural network with three neurons in first hidden layer and two neurons in second hidden layer.

Neuron	Density $\rho$			Errors calculated		
	First hidden layer	Second hidden layer	Output neuron	First hidden layer	Second hidden layer	Output neuron
1	247	1360	5400	-0.04998	-0.10846	0.668582
2	518	876		-0.06411	-0.16845	
3	404			-0.03064		

For a neural network with three neurons in each hidden layer (Fig. 7), the density  $\rho$  and errors calculated in the training process are given in Table 7.

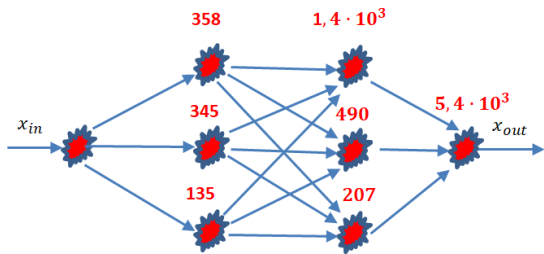


Fig. 7. (Color online) Neural network with three neurons in each hidden layer.

Neuron	Density $\rho$			Errors calculated		
	First hidden layer	Second hidden layer	Output neuron	First hidden layer	Second hidden layer	Output neuron
1	358	1400	5400	-0.01989	-0.0306	0.79636
2	345	490		-0.05095	-0.07231	
3	135	207		-0.05281	-0.20538	

For a neural network with four neurons in the first hidden layer and one neuron in the second hidden layer (Fig. 8), the density  $\rho$  and errors calculated in the training process are given in Table 8.

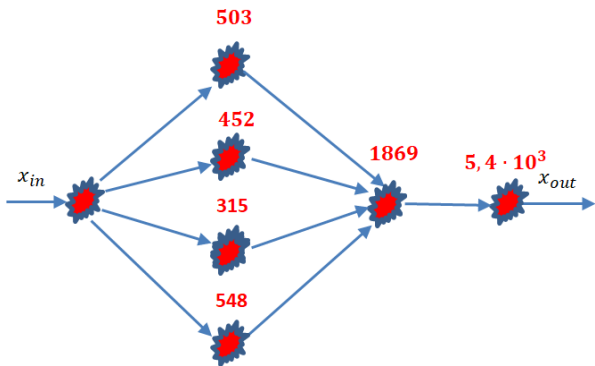


Fig. 8. (Color online) Neural network with four neurons in first hidden layer and one neuron in second hidden layer.

Table 8. Neural network with four neurons in first hidden layer and one neuron in second hidden layer.

Neuron	Density $\rho$			Errors calculated		
	First hidden layer	Second hidden layer	Output neuron	First hidden layer	Second hidden layer	Output neuron
1	503	1869	5400	-0.02634	-0.08973	0.259293
2	452			-0.01514		
3	315			-0.02169		
4	548			-0.02417		

For a neural network with four neurons in the first hidden layer and two neurons in the second hidden layer (Fig. 9), the density  $\rho$  and errors calculated in the training process are given in Table 9.

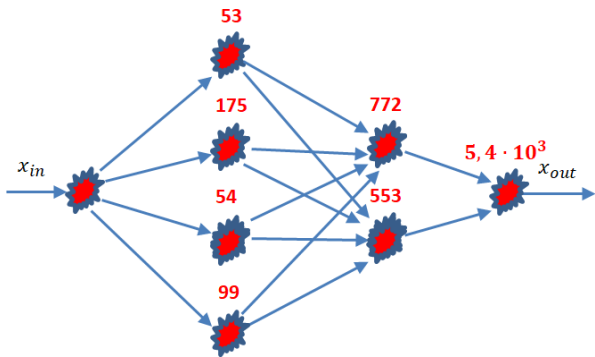


Fig. 9. (Color online) Neural network with four neurons in first hidden layer and two neurons in second hidden layer.

Table 9. Neural network with four neurons in first hidden layer and two neurons in second hidden layer.

Neuron	Density $\rho$			Errors calculated		
	First hidden layer	Second hidden layer	Output neuron	First hidden layer	Second hidden layer	Output neuron
1	53	772	5400	-0.01908	-0.10664	1.039886
2	175	553		-0.01047	-0.14868	
3	54			-0.03368		
4	99			-0.01037		

For a neural network with four neurons in the first hidden layer and three neurons in the second hidden layer (Fig. 10), the density  $\rho$  and errors calculated in the training process are given in Table 10.

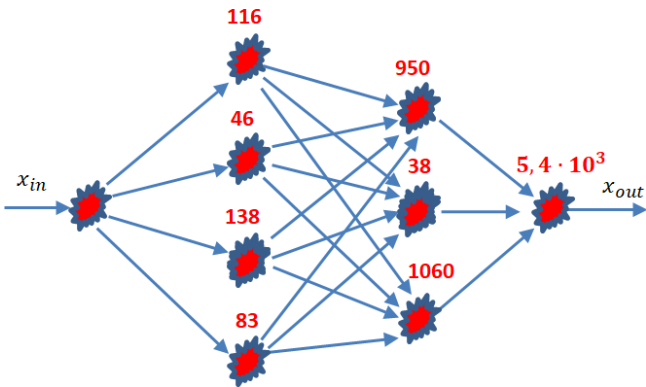


Fig. 10. (Color online) Neural network with four neurons in first hidden layer and three neurons in second hidden layer.

Table 10. Neural network with four neurons in first hidden layer and three neurons in second hidden layer.

Neuron	Density $\rho$			Errors calculated		
	First hidden layer	Second hidden layer	Output neuron	First hidden layer	Second hidden layer	Output neuron
1	116	950	5400	0.013531	0.172603	0.878841
2	46	38		0.02245	-0.0062	
3	138	1060		0.007609	0.154566	
4	83			0.018908		

For a neural network with five neurons in the first hidden layer and one neuron in the second hidden layer (Fig. 11), the density  $\rho$  and errors calculated in the training process are given in Table 11.



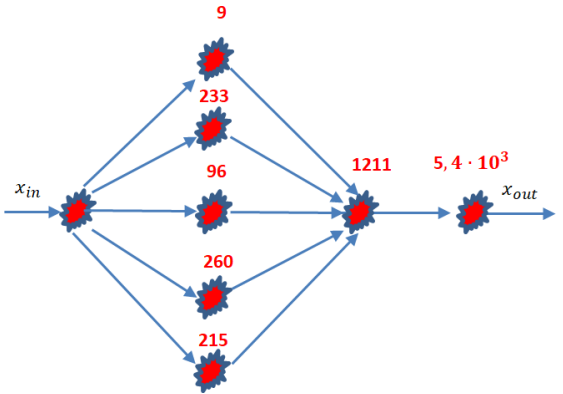


Fig. 11. (Color online) Neural network with five neurons in first hidden layer and one neuron in second hidden layer.

Table 11. Neural network with five neurons in first hidden layer and one neuron in second hidden layer.

Neuron	Density $\rho$			Errors calculated		
	First hidden layer	Second hidden layer	Output neuron	First hidden layer	Second hidden layer	Output neuron
1	9	1211	5400	-0.00089	-0.11623	0.518313
2	233			-0.02236		
3	96			-0.00919		
4	260			-0.02501		
5	215			-0.02066		

For a neural network with five neurons in the first hidden layer and two neurons in the second hidden layer (Fig. 12), the density  $\rho$  and errors calculated in the training process are given in Table 12.

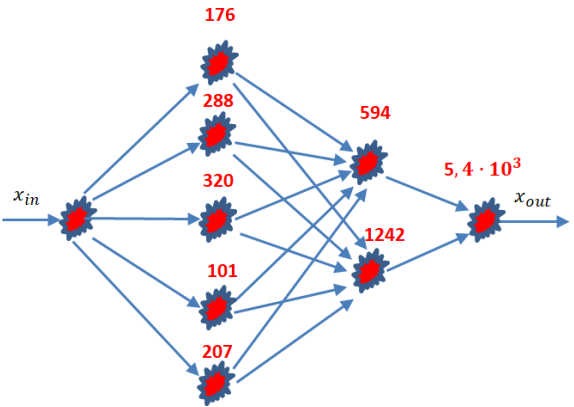


Fig. 12. (Color online) Neural network with five neurons in first hidden layer and two neurons in second hidden layer.

Table 12. Neural network with five neurons in first hidden layer and two neurons in second hidden layer.

Neuron	Density $\rho$			Errors calculated		
	First hidden layer	Second hidden layer	Output neuron	First hidden layer	Second hidden layer	Output neuron
1	176	594	5400	-0.02195	-0.07423	0.674391
2	288	1242		-0.03592	-0.1551	
3	320			-0.03993		
4	101			-0.0126		
5	207			-0.02588		

For a neural network with five neurons in the first hidden layer and three neurons in the second hidden layer (Fig. 13), the density  $\rho$  and errors calculated in the training process are given in Table 13.

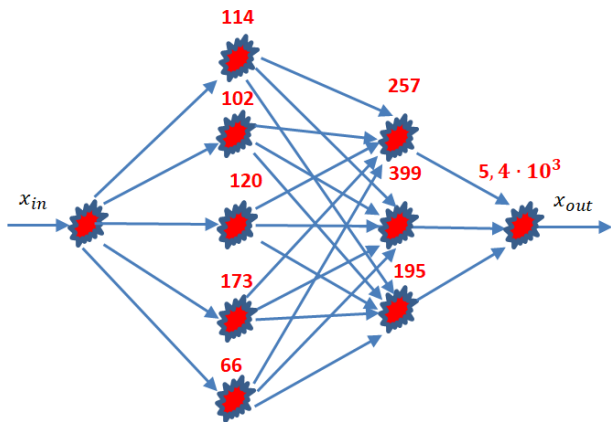


Fig. 13. (Color online) Neural network with five neurons in first hidden layer and three neurons in second hidden layer.

Table 13. Neural network with five neurons in first hidden layer and three neurons in second hidden layer.

Neuron	Density $\rho$			Errors calculated		
	First hidden layer	Second hidden layer	Output neuron	First hidden layer	Second hidden layer	Output neuron
1	114	257	5400	-0.01928	-0.0434	0.911351
2	102	399		-0.01715	-0.06731	
3	120	195		-0.02023	-0.03293	
4	173			-0.02913		
5	66			-0.01118		

For a neural network with five neurons in the first hidden layer and four neurons in the second hidden layer (Fig. 14), the density  $\rho$  and errors calculated in the training process are given in Table 14.

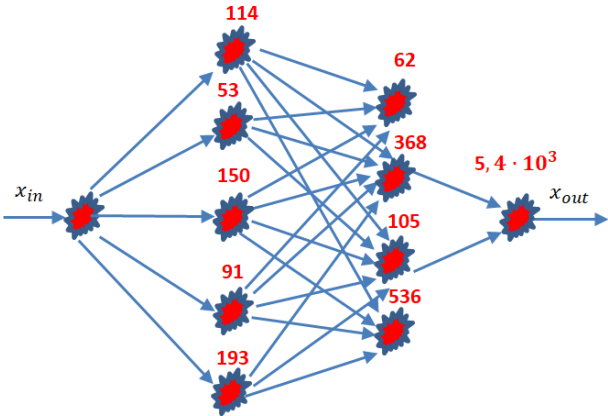


Fig. 14. (Color online) Neural network with five neurons in first hidden layer and four neurons in second hidden layer.

Table 14. Neural network with five neurons in first hidden layer and four neurons in second hidden layer.

Neuron	Density $\rho$			Errors calculated		
	First hidden layer	Second hidden layer	Output neuron	First hidden layer	Second hidden layer	Output neuron
1	114	62	5400	0.018772	0.010128	0.886153
2	53	368		0.008703	0.060393	
3	150	105		0.024637	-0.01725	
4	91	-536		0.014993	0.088012	
5	193			0.031704		

For a neural network with five neurons in each hidden layer (Fig. 15), the density  $\rho$  and errors calculated in the training process are given in Table 15.

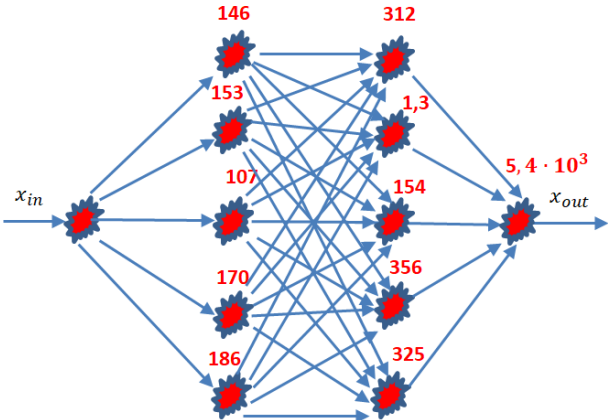


Fig. 15. (Color online) Neural network with five neurons in each hidden layer.

Table 15. Neural network with five neurons in each hidden layer.

Neuron	Density $\rho$			Errors calculated		
	First hidden layer	Second hidden layer	Output neuron	First hidden layer	Second hidden layer	Output neuron
1	146	312	5400	0.022114	0.047203	0.817271
2	153	1300		0.023216	-0.00021	
3	107	154		0.016272	0.023368	
4	170	356		0.025807	0.053826	
5	186	325		0.028239	0.049232	

Based on the neural networks’ application (shown in Figs. 2–15), this original novelty in getting the samples’ surface density, based on a theoretical experiment and neural networks’ calculations, was successfully performed. Collecting the ceramic materials’ densities, from the sample surfaces, based on the neural networks is an advantage in this methodology.<sup>13–20</sup>

4. Outlook

In further researches, we are planning to construct and use neural networks for error calculation and density, where the neural networks are with more neurons in each hidden level, up to 10. This will be the topic of some future research papers.

5. Conclusion

In this paper, we explained the neural network method and its application on the experimental results of bulk density. This novelty is demonstrated on bulk density  $\rho = 5.4 \times 10^3$  [kg/m<sup>3</sup>]. Density values within the different ceramic sample microstructure levels are presented. Instead of an already known stochastic mathematical approach for the calculation of a desired material density, using this approach, we open new frontiers in science of sintering ceramic processing and technology to get the densities within the whole morphology. This advancement is very important when we would like to get exact, precise parameters’ values on the level between the grains and pores, which is important for modern miniaturization demands.

New directions for predicting and designing within the ceramic structure are opened, and we formed the projective structures on quite a precise way. Furthermore, we can also show how this approach<sup>21</sup> could be applied for other parameters’ various calculations in a similar manner.

References

1. D. Rumelhart et al., *Nature* **323** (1986) 533.
2. I. N. da Silva et al., Artificial neural network architectures and training processes, in *Artificial Neural Networks* (Springer, Cham, 2017), pp. 21–28.
3. S. Ribar et al., *Biophys. Rev. Lett.* **16**(1) (2021) 9.

4. R. Hecht-Nielsen, Theory of the backpropagation neural network, in *Int. Joint Conf. Neural Networks*, Vol. 1, Washington DC, USA, 1989, pp. 593–605.
5. V. V. Mitic *et al.*, *Integr. Ferroelectr.* **212** (2020).
6. V. V. Mitic *et al.*, *Mod. Phys. Lett. B* **34**(35) (2020) 2150172.
7. B. Randjelovic *et al.*, *Mod. Phys. Lett. B* **34**(34) (2020) 2150159.
8. V. V. Mitic *et al.*, *Therm. Sci.* **24**(3B) (2020) 2203.
9. V. V. Mitic *et al.*, *Therm. Sci.* (2020) 232.
10. B. Randjelovic *et al.*, Graph theory approach in synthesized diamonds electrophysical parameters defining, in *Bioceramics, Biomimetic and other Compatible Materials Features for Medical Applications* eds. S. Najman, V. Mitic, T. Groth, M. Barbeck, P. Y. Chen and Z. Sun (Springer Nature, Cham, Switzerland, 2021) (accepted for publication).
11. S. Ribar *et al.*, Neural networks from biophysical applications in microelectronics parameters measurements, in *Bioceramics, Biomimetic and other Compatible Materials Features for Medical Applications*, eds. S. Najman, V. Mitic, T. Groth, M. Barbeck, P. Y. Chen and Z. Sun (Springer Nature, Cham, Switzerland, 2021) (accepted for publication).
12. V. V. Mitic, *Structure and Electrical Properties of BaTiO<sub>3</sub> Ceramics* (Zaduzbina Andrejevic, Belgrade, Serbia, 2001) (in Serbian).
13. V. V. Mitić *et al.*, *Int. J. Mod. Phys. B* **35**(7) (2021) 2150103.
14. V. V. Mitić *et al.*, *Ferroelectrics* **570** (2021) 145.
15. V. V. Mitić *et al.*, Fractal microelectronic frontiers and graph theory applications, in *Int. Conf. MS&T 2019*, Book of Abstracts, Portland, USA, 29 September–03 October 2019.
16. V. V. Mitić *et al.*, Investigation of intergranular dielectric properties within the relation between fractal, graph and neural networks theories, in *Int. Conf. Electronic Materials and Applications EMA-2021*, Virtual, 19–21 January 2021.
17. V. V. Mitić *et al.*, Fractal, graph and neural network theories applied on BaTiO<sub>3</sub> electronic ceramics, in *Int. Conf. Electronic Materials and Applications EMA-2021*, Virtual, 19–21 January 2021.
18. V. V. Mitić *et al.*, Neural networks and applied graph theory approaches for intergranular properties measurements investigation, in *Int. Conf. Electronic Materials and Applications EMA-2021*, Virtual, 19–21 January 2021.
19. V. V. Mitić *et al.*, 3D graph theory application on modified nano BaTiO<sub>3</sub> electronic ceramics, in *Int. Conf. Electronic Materials and Applications EMA-2021*, Virtual, 19–21 January 2021.
20. V. V. Mitic *et al.*, *Therm. Sci.* (2021) (accepted).
21. S. Ribar *et al.*, The neural network application on ceramics materials density, in *Int. Conf. IcETRAN 2021*, 8–10 September 2021 (accepted).